

# Model-Free Neural State Estimation in Nonlinear Dynamical Systems: A Comparative Study of Neural Architectures and Classical Filters

Zhuochen Liu<sup>1</sup> Hans Walker<sup>1</sup> Rahul Jain<sup>1</sup>

## Abstract

Neural network models are increasingly used for state estimation in control and decision-making problems, yet it remains unclear to what extent they behave as principled filters in nonlinear dynamical systems. Unlike classical filters, which rely on explicit knowledge of system dynamics and noise models, neural estimators can be trained purely from data without access to the underlying system equations. In this work, we present a systematic empirical comparison between such model-free neural network models and classical filtering methods across multiple nonlinear scenarios. Our study evaluates Transformer-based models, state-space neural networks, and recurrent architectures alongside particle filters and nonlinear Kalman filters. The results show that neural models (in particular, state-space models (SSMs)) achieve state estimation performance that approaches strong nonlinear Kalman filters in nonlinear scenarios and outperform weaker classical baselines despite lacking access to system models, while also attaining substantially higher inference throughput.

## 1. Introduction

Control systems operate under uncertainty due to process noise, sensor noise, and partial observability. In many applications such as robotics, autonomous systems, and cyber-physical systems, the underlying dynamics are nonlinear and the system state cannot be directly observed. Accurate state estimation from noisy and incomplete measurements is therefore a critical component of effective control.

Filtering provides a principled framework for state estimation in such settings. Classical filtering methods explicitly

<sup>1</sup>Ming Hsieh Department of Electrical and Computer Engineering, University of Southern California, Los Angeles, USA. Correspondence to: Zhuochen Liu <liuzhuoc@usc.edu>, Rahul Jain <rahul.jain@usc.edu>.

model system dynamics and observation processes, and use probabilistic inference to recursively estimate latent states. Linear systems with Gaussian noise admit closed-form solutions, while nonlinear systems are commonly addressed using approximate filters. These methods are widely adopted due to their interpretability and strong empirical performance when accurate models are available.

Despite their success, classical filters can struggle in highly nonlinear systems, under model mismatch, or when the dynamics and observation models are only partially known (Judd, 2003; Harlim & Majda, 2008; Berry & Sauer, 2013; Chauchat et al., 2021). These limitations have motivated growing interest in neural network-based approaches to state estimation. Advances in sequence modeling have enabled architectures such as recurrent neural networks, Transformers, and state-space models to achieve strong empirical performance in a variety of estimation and control-related tasks, often without requiring explicit knowledge of system dynamics (Al-Sharman et al., 2019; Zhang et al., 2019; Ghosh et al., 2024; Dahal et al., 2024).

While neural models have shown promising results, their behavior as state estimators is not yet fully understood. In particular, it remains unclear whether these models learn representations that correspond to filtering behavior, or whether their performance reflects statistical regularities specific to the training data. This question is especially relevant in nonlinear dynamical systems and under long-horizon evaluation, where estimation errors can accumulate over time.

A key distinction between classical filtering methods and neural state estimators lies in their informational assumptions. Classical filters rely on explicit system and noise models, and their performance depends critically on the accuracy of these assumptions. In contrast, neural state estimators often operate in a model-free regime and are trained purely from data, without access to the underlying system equations or noise distributions. This raises a natural question: *to what extent can model-free neural state estimators achieve performance comparable to that of model-based classical filters in nonlinear systems where accurate modeling may be difficult or unavailable?*

Several recent works have begun to explore the relation-

ship between neural sequence models and classical filtering methods, including theoretical analyses under specific assumptions on system structure or noise characteristics (Gu et al., 2017; 2021; Monga et al., 2021). While these studies offer useful insights, they are often limited to restricted settings and do not fully characterize practical performance in realistic nonlinear systems.

**Main Contributions.** In this work, we take an empirical approach to addressing these questions. Through controlled experiments across multiple nonlinear dynamical scenarios, we systematically compare neural network models and classical filters as state estimators. Our contributions are summarized as follows: (1) Our systematic empirical comparison between classical filtering methods and a diverse set of neural state estimators, including recurrent networks, Transformer-based models, and structured state-space models (SSMs), shows that neural models perform well without explicit system knowledge. (2) Through controlled training and long-horizon evaluation, we show that state-space models perform consistently well among neural architectures and for most nonlinear systems (except one) approach the performance of strong classical filters. (3) We release the full experimental code used which can be used to verify that the neural models achieve higher inference throughput.

## 2. Related Work

**Classical Filtering and Neural Approximations.** State estimation in dynamical systems has long been studied within the Bayesian filtering framework, with the Kalman filter and its nonlinear extensions forming the backbone of many control and estimation methods (Kalman, 1960). While effective, when accurate models are available, these approaches can degrade under model mismatch or strong nonlinearities, motivating the integration of neural networks into classical filtering pipelines to improve flexibility while retaining recursive structure.

A number of works propose hybrid architectures that combine neural networks with Kalman filtering principles. Recurrent neural networks have been used to learn nonlinear correction terms or gain functions within Kalman-style updates, enabling state estimation when system dynamics are partially known or misspecified (Shaj et al., 2021; Chen et al., 2021; Revach et al., 2022; Choi et al., 2023). Related efforts learn Bayesian filtering steps directly from data without relying on linear-Gaussian assumptions (Lim et al., 2020; Yan et al., 2024). Survey papers provide broader overviews of these hybrid approaches, summarizing their design choices and trade-offs (Jin et al., 2021; Kim et al., 2022; Feng et al., 2023).

**Neural Sequence Models for Filtering.** Beyond hybrid designs, general-purpose sequence models have also been ex-

plored for state estimation. Early empirical studies compare recurrent neural networks with Kalman filters on tracking tasks, with some reporting comparable performance under specific experimental conditions (Chenna et al., 2004; Gao et al., 2019). However, such comparisons are often limited in scope and depend strongly on evaluation assumptions.

More recently, Transformer-based architectures have attracted attention due to their ability to leverage long observation histories. Some work provides a constructive analysis showing that, in linear dynamical systems, a Transformer layer can be designed to approximate the Kalman filter update, establishing a formal connection between self-attention and classical filtering in a restricted setting (Goel & Bartlett, 2024). Complementary empirical studies demonstrate that Transformers trained from data can achieve strong state estimation performance in both linear and nonlinear systems, and can match optimal Kalman filtering in linear cases given sufficient training data (Du et al., 2023). These results are further supported by analyses of sample complexity under specific assumptions.

**Beyond Linear Systems and Alternative Architectures.** Theoretical understanding of neural filtering beyond linear and Markovian systems remains limited. Recent work in continuous-time filtering studies Transformer-like architectures tailored to conditionally Gaussian signal processes, showing that such models can approximate the conditional law of a broad class of nonlinear and non-Markovian systems under noisy observations (Horvath et al., 2025). In parallel, structured sequence models based on state-space formulations have emerged as computationally efficient alternatives to attention-based architectures. Recent work builds neural Kalman filtering frameworks on modern state-space models such as Mamba, targeting nonlinear state estimation with improved efficiency and real-time performance (Gu & Dao, 2024; Sun et al., 2025).

## 3. Preliminaries

### 3.1. Nonlinear Dynamical Systems

We consider discrete-time nonlinear dynamical systems of the form,

$$x_{t+1} = f(x_t, u_t) + w_t, \quad y_t = h(x_t) + v_t, \quad (1)$$

where  $x_t \in \mathbb{R}^n$  denotes the latent system state,  $u_t \in \mathbb{R}^m$  the control input, and  $y_t \in \mathbb{R}^p$  the observation. The functions  $f(\cdot)$  and  $h(\cdot)$  represent nonlinear state transition and observation mappings, respectively, while  $w_t$  and  $v_t$  model process and observation noise. Given a sequence of observations and control inputs, the goal of state estimation is to infer the latent state trajectory  $\{x_t\}$  online. Such nonlinear systems arise naturally in robotics, autonomous driving, and other control problems, where exact Bayesian filtering is

generally intractable and approximate methods are required.

### 3.2. Bayesian Filtering

Bayesian filtering provides a principled framework for sequential state estimation under uncertainty. Given latent states  $\{x_t\}$  and observations  $\{y_t\}$ , the objective is to infer the posterior distribution over the current state conditioned on all past observations and control inputs

$$p(x_t | y_{1:t}, u_{1:t-1}). \quad (2)$$

For the nonlinear state-space model in Equation (1), Bayesian filtering proceeds recursively by propagating the posterior through the dynamics and incorporating new observations. For nonlinear or non-Gaussian systems, the resulting posterior is generally intractable, motivating the use of approximate filtering methods.

### 3.3. Approximate Nonlinear Filtering

Exact Bayesian filtering is tractable only for linear systems with Gaussian noise. For nonlinear systems, a range of approximation methods have been developed. In this work, we consider four widely used nonlinear filters.

The **Extended Kalman Filter (EKF)** applies Kalman filtering to a locally linearized system obtained via first-order Taylor expansions, offering computational efficiency but limited robustness under strong nonlinearities.

The **Unscented Kalman Filter (UKF)** propagates a set of deterministically chosen sigma points through the nonlinear dynamics to better approximate the posterior mean and covariance without explicit linearization.

The **Ensemble Kalman Filter (EnKF)** represents the state distribution using an ensemble of samples and performs updates using sample-based covariance estimates, making it well suited for higher-dimensional systems.

The **Particle Filter (PF)** approximates the posterior using weighted particles and supports general non-Gaussian distributions, at the cost of higher computational expense and potential particle degeneracy.

These methods span different trade-offs between computational efficiency, expressiveness, and robustness, and serve as strong classical baselines for comparison with neural state estimators.

## 4. Experiment Setup

### 4.1. Scenarios

To provide a comprehensive comparison between neural network models and classical filters, we evaluate them on five scenarios with nonlinear dynamics. These scenarios are widely used benchmarks in state estimation and cover

a diverse range of nonlinearities, observation models, and state dimensions.

**Ballistic re-entry.** We use a simplified ballistic re-entry model in which an object falls under gravity through an atmosphere with quadratic drag and an exponential density profile. The state vector is  $\mathbf{x}(t) = [a(t), v(t), c(t)]$ , where  $a(t)$  is altitude above a reference,  $v(t)$  is downward velocity, and  $c(t)$  is a drag/ballistic coefficient treated as part of the state. The continuous-time dynamics are

$$\begin{aligned} \dot{a}(t) &= -v(t), \\ \dot{v}(t) &= g - c(t) v(t)^2 E(a(t)), \\ \dot{c}(t) &= 0, \end{aligned} \quad (3)$$

where  $g > 0$  is gravitational acceleration and

$$E(a) = \min\{\exp(-k a), 1\}$$

models an exponential atmosphere with coefficient  $k > 0$ , clamped to keep drag values reasonable. The state is integrated numerically between discrete observation times using a fixed step integrator (e.g., RK4). At time  $t_k$  an observer measures range to the object with noise:

$$y_k = \sqrt{r_0^2 + (a(t_k) - a_{\text{ref}})^2} + \nu_k, \quad (4)$$

where  $r_0 > 0$  is a fixed horizontal offset,  $a_{\text{ref}}$  is a reference altitude, and  $\nu_k$  is measurement noise. This model is a standard simplified entry model with exponential air density and quadratic drag.

**Bearings-only tracking.** We consider 2D single-sensor bearings-only target tracking (BOT) with a constant-velocity motion model (Scala & Morelande, 2008). The state is  $\mathbf{x}_k = [p_{x,k}, p_{y,k}, v_{x,k}, v_{y,k}]$  with discrete dynamics

$$\mathbf{x}_{k+1} = \begin{bmatrix} 1 & 0 & T & 0 \\ 0 & 1 & 0 & T \\ 0 & 0 & 1 & 0 \\ 0 & 0 & 0 & 1 \end{bmatrix} \mathbf{x}_k + \mathbf{w}_k, \quad (5)$$

where  $T$  is the sampling period and  $\mathbf{w}_k$  is process noise. The observation is the bearing from the origin to the target,

$$y_k = \text{wrap}(\arctan 2(p_{y,k}, p_{x,k})) + \nu_k, \quad (6)$$

where  $\arctan 2(\cdot, \cdot)$  returns an angle in  $(-\pi, \pi]$ ,  $\text{wrap}(\cdot)$  maps angles to  $(-\pi, \pi]$ , and  $\nu_k$  is measurement noise. As is well-known in single-sensor BOT, the problem can be ill-conditioned (e.g., weak range observability) without informative geometry / maneuvering or careful initialization (Scala & Morelande, 2008).

**Lorenz 96.** The Lorenz 96 system (Lorenz, 1996) is a standard chaotic testbed for data assimilation and filtering,

consisting of  $J$  coupled ODEs arranged on a cyclic index

$$\frac{dX_j}{dt} = (X_{j+1} - X_{j-2})X_{j-1} - X_j + F, \quad (7)$$

$$j = 1, \dots, J.$$

with cyclic boundary conditions  $X_{-1} = X_{J-1}$ ,  $X_0 = X_J$ , and  $X_{J+1} = X_1$ . The forcing parameter  $F$  controls the regime; common choices (e.g.,  $F \approx 8$ ) yield strongly chaotic dynamics.

**N-link pendulum.** The  $N$ -link pendulum consists of  $N$  rigid links of lengths  $R_1, \dots, R_N$  with point masses  $m_1, \dots, m_N$  at their endpoints, connected serially in a planar configuration. Let  $\theta_j$  denote the angle of link  $j$  from the vertical and  $\omega_j = \dot{\theta}_j$  its angular velocity. The Lagrangian for the  $i$ th mass can be written in terms of kinetic and potential energy contributions as

$$\mathcal{L}_i(\theta, \omega) = \frac{1}{2} m_i \sum_{j=1}^i \sum_{k=1}^i R_j R_k \omega_j \omega_k \cos(\theta_j - \theta_k) \quad (8)$$

$$+ m_i g \sum_{j=1}^i R_j \cos(\theta_j),$$

where  $g$  is gravitational acceleration. The full system Lagrangian is the sum over links,

$$\mathcal{L}(\theta, \omega) = \sum_{i=1}^N \mathcal{L}_i(\theta, \omega),$$

The resulting equations of motions, found via the Euler Lagrange Equations, define the nonlinear coupled dynamics. This system exhibits strong nonlinear coupling and sensitivity to initial conditions, making it the most challenging benchmark we test.

**Planar Quadrotor.** The planar quadrotor scenario (Singh et al., 2023) considers a quadrotor constrained to motion within a two-dimensional vertical plane. The system is modeled in discrete time with a six-dimensional state vector  $\mathbf{x}_t = [x_t, z_t, \phi_t, \dot{x}_t, \dot{z}_t, \dot{\phi}_t]$ . The full discrete-time state transition dynamics are given by

$$\mathbf{x}_{t+1} = \begin{bmatrix} x_t + (\dot{x}_t \cos \phi_t - \dot{z}_t \sin \phi_t) \tau \\ z_t + (\dot{x}_t \sin \phi_t + \dot{z}_t \cos \phi_t) \tau \\ \phi_t + \dot{\phi}_t \tau \\ \dot{x}_t + (\dot{z}_t \dot{\phi}_t - g \sin \phi_t) \tau \\ \dot{z}_t + (-\dot{x}_t \dot{\phi}_t - g \cos \phi_t + (u_{0,t} + u_{1,t})/m) \tau \\ (u_{0,t} - u_{1,t}) l \tau / J \end{bmatrix} + \mathbf{w}_t, \quad (9)$$

$$\mathbf{y}_t = \mathbf{C} \mathbf{x}_t + \mathbf{v}_t,$$

where  $\mathbf{w}_t$  and  $\mathbf{v}_t$  denote process and observation noise, respectively, and the observation matrix  $\mathbf{C} \in \mathbb{R}^{3 \times 6}$  is sampled

once with entries drawn independently from a uniform distribution on  $[0, 1]$ . Although  $\mathbf{C}$  represents a randomly generated linear mapping from states to observations, it is fixed throughout training and evaluation to ensure a well-defined and meaningful learning task.

The system captures the essential coupling between translational motion and rotational dynamics of an aerial vehicle, while remaining low-dimensional and computationally tractable. Due to gravity and the coupling between attitude and thrust, the system is inherently unstable in open loop and exhibits strongly nonlinear behavior. In our experiments, we use the same physical parameters as in Du et al. (2023) to ensure consistency with prior work, while increasing the observation noise standard deviation from 0.01 to 0.1 to more rigorously evaluate robustness.

## 4.2. Models

We evaluate a range of neural architectures as state estimators, spanning three widely used model families. Specifically, we benchmark six models. For the prevailing *Transformer-based approaches*, we consider GPT-2 (Radford et al., 2019) and Filterformer (Horvath et al., 2025). For the emerging *structured state-space models (SSMs)*, we include Mamba (Gu & Dao, 2024) and its successor, Mamba-2 (Dao & Gu, 2024). We also evaluate recurrent neural networks commonly used in control settings, namely GRU (Cho et al., 2014) and LSTM (Hochreiter & Schmidhuber, 1997).

In our experiments, all models are configured to have approximately 100,000 parameters. This parameter scale is chosen to avoid trivial underparameterization while remaining computationally efficient, and we use the same parameter scale across architectures to ensure a fair comparison. In addition, all neural models are trained and evaluated without access to the system dynamics, observation functions, or noise parameters used by classical filters.

## 4.3. Training Setup

To assess model robustness to dataset realizations, each scenario uses three independently generated training datasets. To evaluate sensitivity to parameter initialization, five models are trained on each dataset. All trained models are evaluated independently, and performance variability is reported across all 15 runs.

Each training dataset consists of 20,000 trajectories with a horizon length of 100, yielding a total of 2,000,000 tokens and a data-to-parameter ratio of approximately 20:1. Training samples are obtained by randomly extracting subtrajectories from longer trajectories of length 500, which helps improve coverage of the underlying data distribution.

For each training dataset, an independent validation set of

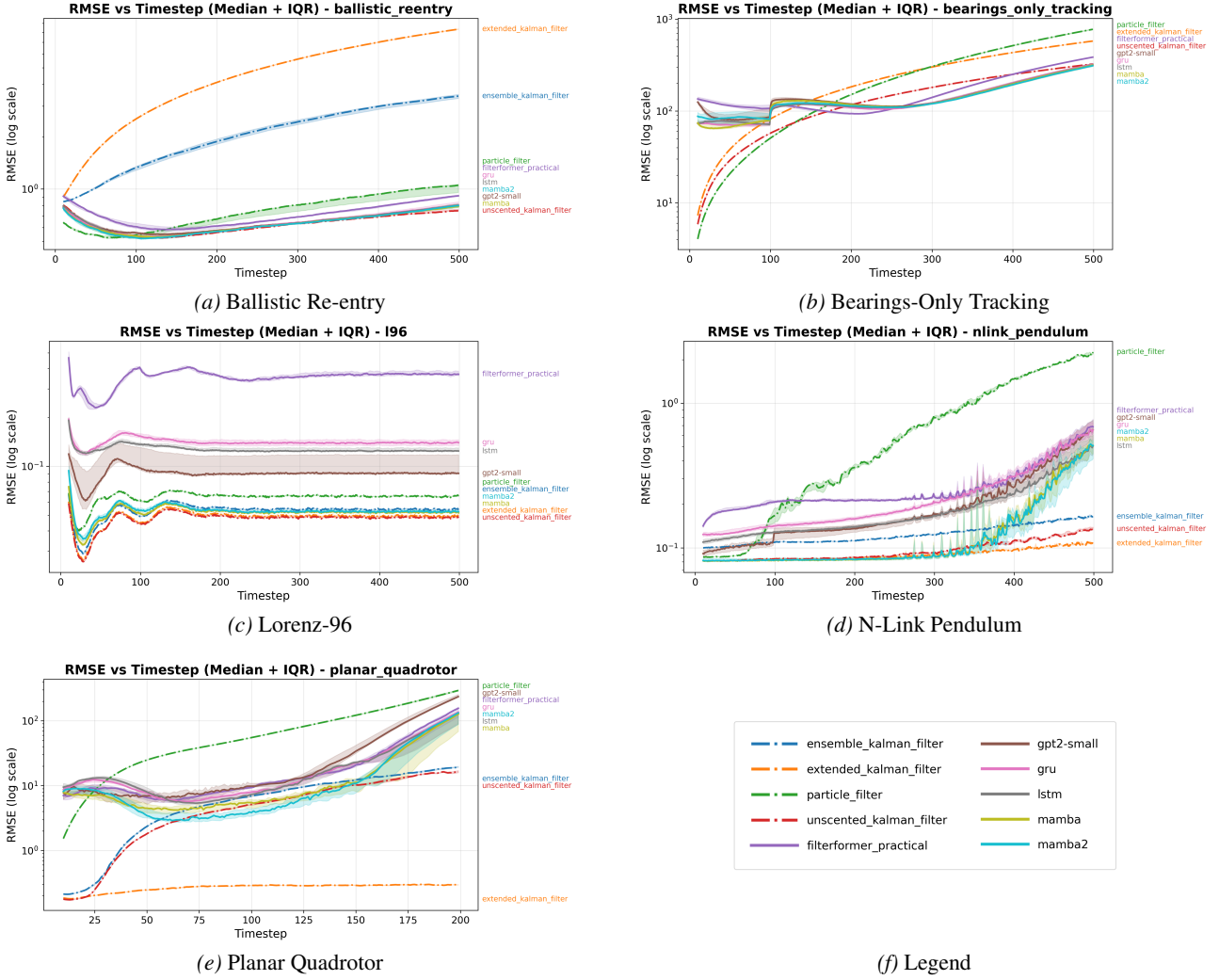


Figure 1. RMSE as a function of timestep across the five scenarios. Curves show median error across runs, with shaded regions indicating interquartile ranges. A shared legend is shown in the bottom-right panel. EnKF is omitted from the Bearings-Only Tracking scenario due to divergence.

8,000 trajectories is generated and used for early stopping to mitigate overfitting. The validation trajectories follow the same chunking procedure and horizon length as the training data.

#### 4.4. Evaluation Setup

To evaluate model and filter performance, each scenario uses three independent evaluation datasets. Each dataset consists of 8,000 trajectories with a horizon length of 500. Training on shorter trajectories while evaluating on longer trajectories is intended to assess whether models learn the underlying filtering behavior, rather than simply memorizing trajectory-specific patterns.

The only exception is the Planar Quadrotor scenario, which is evaluated with a horizon length of 200. Without appropriate control inputs, the quadrotor undergoes free fall, causing

the  $z$ -axis state to grow unbounded over time. Consequently, estimation errors accumulate and eventually diverge, making long-horizon evaluation uninformative. Following the setup of Du et al. (2023), we therefore use a horizon length of 200 for this scenario.

#### 4.5. Evaluation Metrics

To facilitate interpretation of model and filter performance as state estimators, we report Root Mean Square Error (RMSE) as a function of timestep. Results are summarized using the median estimation error with interquartile ranges across runs, providing a robust characterization of typical performance under long-horizon evaluation.

To assess robustness to observation noise, we additionally report average RMSE under varying Signal-to-Noise Ratio (SNR) levels, with SNR measured in decibels.

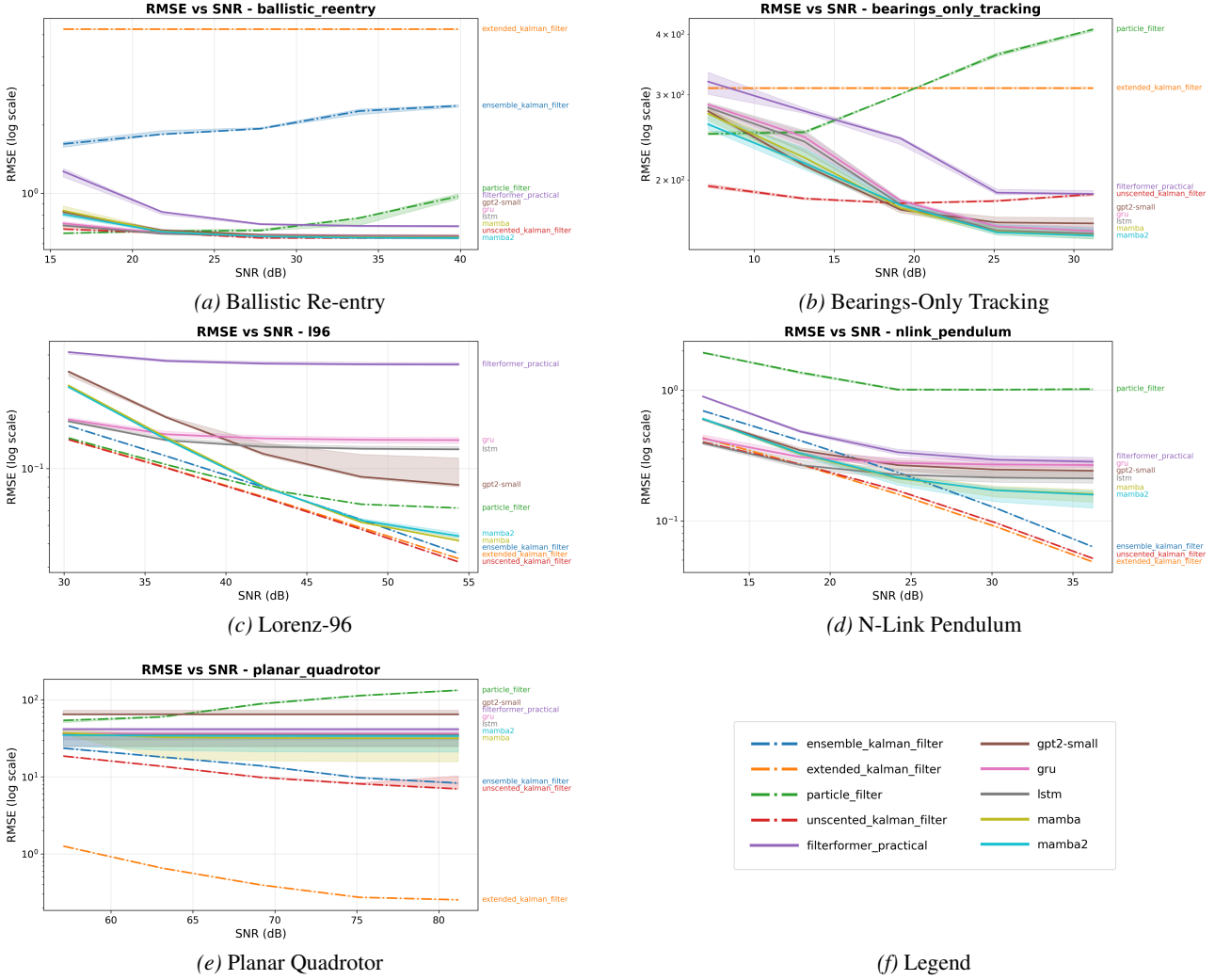


Figure 2. RMSE under varying observation noise levels across the five scenarios. EnKF is omitted from the Bearings-Only Tracking scenario due to divergence.

For a more comprehensive evaluation, we report aggregated metrics including average RMSE over the full trajectory, Mean Absolute Error (MAE), Median Absolute Error (MedAE), normalized RMSE (NRMSE), the area under the RMSE–timestep curve (AUC), and runtime performance. For completeness, we also include average RMSE reported with the mean and 95% confidence intervals in the full metrics table provided in the Appendix.

## 5. Results

We evaluate neural network models and classical filters across five nonlinear dynamical scenarios using the metrics described in Section 4.5. Results are reported over multiple independently generated datasets and random initializations, and summarized using the median across runs with interquartile ranges unless otherwise noted.

### 5.1. RMSE over Time

Figure 1 shows the Root Mean Square Error (RMSE) as a function of timestep for all methods and scenarios. Each subplot corresponds to one scenario, with curves showing median error across runs and shaded regions indicating interquartile ranges. These plots illustrate both estimation accuracy and error evolution under long-horizon evaluation.

### 5.2. Aggregated Performance Metrics

Tables 1–5 report aggregated long-horizon metrics for each method and scenario, including average RMSE, MAE, MedAE, normalized RMSE (NRMSE), and the area under the RMSE–timestep curve (AUC). These metrics enable direct quantitative comparison across methods within each scenario. For brevity, only median values are reported here, with full median  $\pm$  IQR statistics provided in the Appendix.

Table 1. Aggregated state estimation metrics for the Ballistic Reentry scenario. Values are reported as median across runs.

Method	RMSE	MAE	MedAE	NRMSE	AUC
<i>Classical Filters</i>					
EKF	5.283	3.002	0.903	1.568	2364.2
UKF	<b>0.634</b>	<b>0.362</b>	0.154	<b>0.605</b>	<b>307.9</b>
EnKF	2.303	0.587	0.160	0.896	1060.9
PF	0.778	0.366	<b>0.145</b>	0.643	371.4
<i>Neural Models</i>					
GRU	0.647	0.390	0.202	0.605	313.7
LSTM	0.645	0.386	0.200	0.607	312.8
GPT-2	0.650	0.396	0.208	0.610	315.6
Filterformer	0.718	0.445	0.250	0.669	348.1
Mamba	0.638	0.380	0.189	0.600	309.3
Mamba-2	<b>0.636</b>	<b>0.371</b>	<b>0.182</b>	<b>0.599</b>	<b>307.6</b>

Table 2. Aggregated state estimation metrics for the Bearings Only Tracking scenario. Values are reported as median across runs.

Method	RMSE	MAE	MedAE	NRMSE	AUC
<i>Classical Filters</i>					
EKF	309.764	147.864	4.458	1.009	127666.6
UKF	<b>180.981</b>	<b>73.284</b>	<b>2.730</b>	<b>0.648</b>	<b>76311.0</b>
EnKF	$\infty$	$\infty$	$\infty$	$\infty$	$\infty$
PF	363.150	108.129	4.146	1.418	138321.6
<i>Neural Models</i>					
GRU	160.496	70.828	2.675	0.549	70850.0
LSTM	157.315	70.299	2.632	0.537	69968.6
GPT-2	163.471	74.504	2.755	0.563	73587.8
Filterformer	188.368	84.899	3.152	0.648	81846.1
Mamba	156.477	<b>69.142</b>	<b>2.631</b>	0.540	<b>69624.0</b>
Mamba-2	<b>155.987</b>	70.550	2.649	<b>0.536</b>	70442.7

Table 3. Aggregated state estimation metrics for the L96 scenario. Values are reported as median across runs.

Method	RMSE	MAE	MedAE	NRMSE	AUC
<i>Classical Filters</i>					
EKF	0.049	0.027	0.013	0.014	23.7
UKF	<b>0.048</b>	<b>0.026</b>	<b>0.013</b>	<b>0.013</b>	<b>23.2</b>
EnKF	0.054	0.029	0.013	0.015	26.1
PF	0.065	0.037	0.018	0.018	31.6
<i>Neural Models</i>					
GRU	0.142	0.110	0.090	0.040	69.3
LSTM	0.127	0.099	0.082	0.036	62.2
GPT-2	0.090	0.069	0.057	0.026	44.1
Filterformer	0.356	0.252	0.177	0.101	173.2
Mamba	<b>0.052</b>	<b>0.031</b>	<b>0.017</b>	<b>0.015</b>	<b>25.3</b>
Mamba-2	0.053	0.032	0.018	0.015	25.9

Table 4. Aggregated state estimation metrics for the Nlink Pendulum scenario. Values are reported as median across runs.

Method	RMSE	MAE	MedAE	NRMSE	AUC
<i>Classical Filters</i>					
EKF	<b>0.090</b>	<b>0.069</b>	<b>0.057</b>	<b>0.030</b>	<b>44.1</b>
UKF	0.097	0.070	0.058	0.031	46.7
EnKF	0.125	0.092	0.073	0.041	60.7
PF	1.008	0.188	0.066	0.311	378.2
<i>Neural Models</i>					
GRU	0.270	0.154	0.110	0.084	115.9
LSTM	0.214	0.126	0.097	0.066	93.3
GPT-2	0.247	0.128	0.094	0.075	101.0
Filterformer	0.294	0.156	0.111	0.093	132.4
Mamba	0.172	<b>0.070</b>	<b>0.058</b>	<b>0.051</b>	66.7
Mamba-2	<b>0.171</b>	0.071	0.058	0.052	<b>65.3</b>

Table 5. Aggregated state estimation metrics for the Planar Quadrotor scenario. Values are reported as median across runs.

Method	RMSE	MAE	MedAE	NRMSE	AUC
<i>Classical Filters</i>					
EKF	<b>0.273</b>	<b>0.125</b>	<b>0.041</b>	<b>0.007</b>	<b>51.2</b>
UKF	8.112	0.988	0.054	0.068	1223.4
EnKF	9.726	1.738	0.092	0.083	1501.8
PF	113.424	38.262	1.302	0.898	16098.9
<i>Neural Models</i>					
GRU	36.423	6.305	1.562	0.201	4330.8
LSTM	35.205	6.275	1.381	0.198	4223.1
GPT-2	64.994	8.082	1.864	0.239	6873.7
Filterformer	41.504	7.308	1.562	0.225	4672.7
Mamba	<b>31.768</b>	2.995	0.635	0.164	<b>3327.6</b>
Mamba-2	33.925	<b>2.614</b>	<b>0.573</b>	<b>0.159</b>	3334.1

Table 6. Runtime performance in iterations per second (iter/s). Higher is better.

Method	Ballistic	Bearings	L96	N-Link	Quad.
<i>Classical Filters</i>					
EKF	96.0	855.9	143.1	193.4	611.5
UKF	244.4	706.7	407.1	181.9	624.4
EnKF	<b>369.7</b>	<b>1748.1</b>	<b>612.7</b>	<b>218.1</b>	<b>1400.4</b>
PF	303.9	1292.1	514.3	178.8	937.3
<i>Neural Models</i>					
GRU	<b>4029.9</b>	5184.4	4926.7	<b>4721.8</b>	<b>5861.5</b>
LSTM	3965.7	<b>5203.8</b>	<b>4945.4</b>	4694.8	5759.3
GPT-2	577.0	833.7	825.5	807.4	1176.8
Filterformer	2065.7	2344.6	2461.9	2430.0	3204.8
Mamba	1645.2	2094.5	2066.8	2005.9	2751.0
Mamba-2	632.1	812.1	808.7	791.3	1155.7

### 5.3. Robustness to Observation Noise

Figure 2 reports RMSE under varying observation noise levels for each scenario. Results are shown separately to highlight system-dependent sensitivity to noise. Neural models are evaluated at noise levels up to eight times higher than those seen during training, providing a stringent robustness test.

### 5.4. Runtime Performance

Table 6 reports average runtime per timestep for all methods, measured on GPU and reported in iterations per second (iter/s). Runtime is reported independently of estimation accuracy to facilitate direct comparison of computational efficiency across methods.

### 5.5. Observations

We summarize several consistent trends observed across scenarios, metrics, and evaluation settings.

1. **State-space models perform consistently well among neural architectures.** Across all scenarios, state-space neural models, namely Mamba and Mamba-2, exhibit strong and stable performance relative to other neural architectures, often outperforming recurrent and Transformer-based models under identical protocols.
2. **State-space models approach the performance of strong classical filters.** State-space neural models achieve estimation accuracy close to that of strong model-based filters such as the EKF and UKF, with a substantially smaller performance gap than other neural architectures, particularly in scenarios with unstructured observation models.
3. **Neural models perform well without explicit system knowledge.** All neural estimators operate in a model-free regime without access to system dynamics or noise models, yet recover a significant fraction of the performance of model-based classical filters across nonlinear systems.
4. **Neural models achieve higher inference throughput.** Neural models consistently achieve higher inference throughput than classical filtering methods across all scenarios, highlighting their practical advantages in real-time or resource-constrained settings.

## 6. Conclusions

We presented a systematic empirical comparison between neural network models and classical filtering methods for state estimation in nonlinear dynamical systems. Using a

unified experimental framework, we evaluated a diverse set of neural architectures and established filters across multiple nonlinear scenarios, long-horizon rollouts, and varying levels of observation noise.

Our results show that neural sequence models trained purely from data can act as effective state estimators in a range of nonlinear settings. Despite operating in a model-free regime without access to system dynamics or noise models, neural estimators recover a substantial fraction of the performance of strong model-based nonlinear filters, while significantly outperforming weaker or mismatched classical baselines. Moreover, neural models consistently achieve much higher inference throughput than classical filtering methods, highlighting their practical advantages in computationally constrained settings.

Overall, this study provides empirical evidence that data-driven models can exhibit filtering-like behavior in the sense of stable and accurate long-horizon state estimation, while also clarifying conditions under which classical filters remain preferable when accurate system models are available. We hope that the benchmarks and results presented here help inform future work at the intersection of control, filtering, and sequence modeling.

**Limitations.** Although neural estimators operate in a model-free regime, they rely on supervised training data. In our experiments, the training scale corresponds to a data-to-parameter ratio of approximately 20:1 when measured in observed timesteps, which may still be impractical in data-scarce control applications. In addition, our evaluation focuses on point estimation accuracy and does not assess uncertainty calibration or posterior quality, nor does it explicitly distinguish filtering from smoothing behavior or analyze strict causality and belief compression properties. Finally, performance can be sensitive to both model architecture and experimental setup, motivating further study of data efficiency, architectural inductive biases, and robustness across a broader class of systems.

## Impact Statement

This paper presents work whose goal is to advance the field of Machine Learning. There are many potential societal consequences of our work, none of which we feel must be specifically highlighted here.

## References

Al-Sharman, M. K., Zweiri, Y., Jaradat, M. A. K., Al-Husari, R., Gan, D., and Seneviratne, L. D. Deep-learning-based neural network training for state estimation enhancement: Application to attitude estimation. *IEEE Transactions on Instrumentation and Measurement*, 69(1):24–34, 2019.

Berry, T. and Sauer, T. Adaptive ensemble kalman filtering of non-linear systems. *Tellus A: Dynamic Meteorology and Oceanography*, 65(1):20331, 2013.

Chauchat, P., Vilà-Valls, J., and Chaumette, E. Robust information filtering under model mismatch for large-scale dynamic systems. *IEEE Control Systems Letters*, 6: 818–823, 2021.

Chen, C., Lu, C. X., Wang, B., Trigoni, N., and Markham, A. Dynanet: Neural kalman dynamical model for motion estimation and prediction. *IEEE Transactions on Neural Networks and Learning Systems*, 32(12):5479–5491, 2021.

Chenna, S. K., Jain, Y. K., Kapoor, H., Bapi, R. S., Yadaiah, N., Negi, A., Rao, V. S., and Deekshatulu, B. L. State estimation and tracking problems: A comparison between kalman filter and recurrent neural networks. In *International Conference on Neural Information Processing*, pp. 275–281. Springer, 2004.

Cho, K., Van Merriënboer, B., Gulcehre, C., Bahdanau, D., Bougares, F., Schwenk, H., and Bengio, Y. Learning phrase representations using rnn encoder-decoder for statistical machine translation. *arXiv preprint arXiv:1406.1078*, 2014.

Choi, G., Park, J., Shlezinger, N., Eldar, Y. C., and Lee, N. Split-kalmannet: A robust model-based deep learning approach for state estimation. *IEEE transactions on vehicular technology*, 72(9):12326–12331, 2023.

Dahal, P., Mentasti, S., Paparusso, L., Arrigoni, S., and Braghin, F. Robuststatenet: Robust ego vehicle state estimation for autonomous driving. *Robotics and Autonomous Systems*, 172:104585, 2024.

Dao, T. and Gu, A. Transformers are ssms: Generalized models and efficient algorithms through structured state space duality. *arXiv preprint arXiv:2405.21060*, 2024.

Du, Z., Balim, H., Oymak, S., and Ozay, N. Can transformers learn optimal filtering for unknown systems? *IEEE Control Systems Letters*, 7:3525–3530, 2023.

Feng, S., Li, X., Zhang, S., Jian, Z., Duan, H., and Wang, Z. A review: State estimation based on hybrid models of kalman filter and neural network. *Systems Science & Control Engineering*, 11(1):2173682, 2023.

Gao, C., Yan, J., Zhou, S., Varshney, P. K., and Liu, H. Long short-term memory-based deep recurrent neural networks for target tracking. *Information Sciences*, 502:279–296, 2019.

Ghosh, A., Honoré, A., and Chatterjee, S. Danse: Data-driven non-linear state estimation of model-free process in unsupervised learning setup. *IEEE transactions on signal processing*, 72:1824–1838, 2024.

Goel, G. and Bartlett, P. Can a transformer represent a kalman filter? In *6th Annual Learning for Dynamics & Control Conference*, pp. 1502–1512. PMLR, 2024.

Gu, A. and Dao, T. Mamba: Linear-time sequence modeling with selective state spaces. In *First conference on language modeling*, 2024.

Gu, A., Johnson, I., Goel, K., Saab, K., Dao, T., Rudra, A., and Ré, C. Combining recurrent, convolutional, and continuous-time models with linear state space layers. *Advances in neural information processing systems*, 34: 572–585, 2021.

Gu, J., Yang, X., De Mello, S., and Kautz, J. Dynamic facial analysis: From bayesian filtering to recurrent neural network. In *Proceedings of the IEEE conference on computer vision and pattern recognition*, pp. 1548–1557, 2017.

Harlim, J. and Majda, A. Filtering nonlinear dynamical systems with linear stochastic models. *Nonlinearity*, 21 (6):1281, 2008.

Hochreiter, S. and Schmidhuber, J. Long short-term memory. *Neural computation*, 9(8):1735–1780, 1997.

Horvath, B., Kratsios, A., Limmer, Y., and Yang, X. Transformers can solve non-linear and non-markovian filtering problems in continuous time for conditionally gaussian signals, 2025. URL <https://arxiv.org/abs/2310.19603>.

Jin, X.-B., Robert Jeremiah, R. J., Su, T.-L., Bai, Y.-T., and Kong, J.-L. The new trend of state estimation: From model-driven to hybrid-driven methods. *Sensors*, 21(6): 2085, 2021.

Judd, K. Nonlinear state estimation, indistinguishable states, and the extended kalman filter. *Physica D: Nonlinear Phenomena*, 183(3-4):273–281, 2003.

Kalman, R. E. A new approach to linear filtering and prediction problems. *Transactions of the ASME-Journal of Basic Engineering*, 82(1):35–45, 1960. doi: 10.1115/1.3662552.

Kim, S., Petrunin, I., and Shin, H.-S. A review of kalman filter with artificial intelligence techniques. In *2022 Integrated Communication, Navigation and Surveillance Conference (ICNS)*, pp. 1–12. IEEE, 2022.

Lim, B., Zohren, S., and Roberts, S. Recurrent neural filters: Learning independent bayesian filtering steps for time series prediction. In *2020 International Joint Conference on Neural Networks (IJCNN)*, pp. 1–8. IEEE, 2020.

Lorenz, E. N. Predictability: A problem partly solved. In *Seminar on Predictability*, Reading, United Kingdom, 1996. European Centre for Medium-Range Weather Forecasts (ECMWF).

Monga, V., Li, Y., and Eldar, Y. C. Algorithm unrolling: Interpretable, efficient deep learning for signal and image processing. *IEEE Signal Processing Magazine*, 38(2):18–44, 2021.

Radford, A., Wu, J., Child, R., Luan, D., Amodei, D., Sutskever, I., et al. Language models are unsupervised multitask learners. *OpenAI blog*, 1(8):9, 2019.

Revach, G., Shlezinger, N., Ni, X., Escoriza, A. L., Van Sloun, R. J., and Eldar, Y. C. Kalmannet: Neural network aided kalman filtering for partially known dynamics. *IEEE Transactions on Signal Processing*, 70:1532–1547, 2022.

Scala, B. F. L. and Morelande, M. R. An analysis of the single sensor bearings-only tracking problem. In *11th International Conference on Information Fusion (FUSION 2008), Cologne, Germany, June 30–July 3, 2008*, pp. 1–6. IEEE, 2008. doi: 10.1109/ICIF.2008.4632255. URL <https://ieeexplore.ieee.org/document/4632255/>.

Shaj, V., Becker, P., Büchler, D., Pandya, H., van Duijkeren, N., Taylor, C. J., Hanheide, M., and Neumann, G. Action-conditional recurrent kalman networks for forward and inverse dynamics learning. In *Conference on Robot Learning*, pp. 765–781. PMLR, 2021.

Singh, S., Landry, B., Majumdar, A., Slotine, J.-J., and Pavone, M. Robust feedback motion planning via contraction theory. *The International Journal of Robotics Research*, 42(9):655–688, 2023.

Sun, J., Shen, J., Tong, J., Tang, T., Yin, Y., Ohtsuki, T., and Gui, G. Towards robust and real-time state estimation: A neural kalman filter framework with mamba architecture. *IEEE Transactions on Vehicular Technology*, 2025.

Yan, S., Liang, Y., Zheng, L., Fan, M., Wang, X., and Wang, B. Explainable gated bayesian recurrent neural network for non-markov state estimation. *IEEE Transactions on Signal Processing*, 72:4302–4317, 2024.

Zhang, L., Wang, G., and Giannakis, G. B. Real-time power system state estimation and forecasting via deep unrolled neural networks. *IEEE Transactions on Signal Processing*, 67(15):4069–4077, 2019.

## A. Full Evaluation Metrics

Tables 7–11 report detailed metrics for each method across all scenarios, including the full median  $\pm$  IQR values as well as the mean  $\pm$  95% confidence interval of the averaged RMSE.

Table 7. Extended metrics for Ballistic Reentry. Values: median $\pm$ IQR, last column: mean $\pm$ 95%CI.

Method	RMSE	MAE	MedAE	NRMSE	AUC	RMSE (mean $\pm$ 95%CI)
<i>Classical Filters</i>						
EKF	5.283 $\pm$ 0.030	3.002 $\pm$ 0.015	0.903 $\pm$ 0.001	1.568 $\pm$ 0.003	2364.2 $\pm$ 12.1	5.288 $\pm$ 0.076
UKF	<b>0.634<math>\pm</math>0.007</b>	<b>0.362<math>\pm</math>0.001</b>	0.154 $\pm$ 0.000	<b>0.605<math>\pm</math>0.002</b>	<b>307.9<math>\pm</math>3.0</b>	<b>0.635<math>\pm</math>0.017</b>
EnKF	2.303 $\pm$ 0.126	0.587 $\pm$ 0.017	0.160 $\pm$ 0.000	0.896 $\pm$ 0.013	1060.9 $\pm$ 57.1	2.282 $\pm$ 0.316
PF	0.778 $\pm$ 0.058	0.366 $\pm$ 0.004	<b>0.145<math>\pm</math>0.000</b>	0.643 $\pm$ 0.015	371.4 $\pm$ 25.8	0.743 $\pm$ 0.162
<i>Neural Models</i>						
GRU	0.647 $\pm$ 0.020	0.390 $\pm$ 0.010	0.202 $\pm$ 0.015	0.605 $\pm$ 0.011	313.7 $\pm$ 9.1	0.649 $\pm$ 0.007
LSTM	0.645 $\pm$ 0.015	0.386 $\pm$ 0.016	0.200 $\pm$ 0.016	0.607 $\pm$ 0.009	312.8 $\pm$ 7.6	0.646 $\pm$ 0.005
GPT-2	0.650 $\pm$ 0.011	0.396 $\pm$ 0.013	0.208 $\pm$ 0.018	0.610 $\pm$ 0.008	315.6 $\pm$ 4.5	0.650 $\pm$ 0.005
Filterformer	0.718 $\pm$ 0.011	0.445 $\pm$ 0.022	0.250 $\pm$ 0.026	0.669 $\pm$ 0.022	348.1 $\pm$ 6.6	0.717 $\pm$ 0.006
Mamba	0.638 $\pm$ 0.011	0.380 $\pm$ 0.013	0.189 $\pm$ 0.016	0.600 $\pm$ 0.006	309.3 $\pm$ 5.5	0.639 $\pm$ 0.005
Mamba-2	<b>0.636<math>\pm</math>0.010</b>	<b>0.371<math>\pm</math>0.013</b>	<b>0.182<math>\pm</math>0.015</b>	<b>0.599<math>\pm</math>0.008</b>	<b>307.6<math>\pm</math>4.9</b>	<b>0.638<math>\pm</math>0.006</b>

Table 8. Extended metrics for Bearings Only Tracking. Values: median $\pm$ IQR, last column: mean $\pm$ 95%CI.

Method	RMSE	MAE	MedAE	NRMSE	AUC	RMSE (mean $\pm$ 95%CI)
<i>Classical Filters</i>						
EKF	309.764 $\pm$ 2.329	147.864 $\pm$ 0.851	4.458 $\pm$ 0.030	1.009 $\pm$ 0.000	127666.6 $\pm$ 953.1	309.679 $\pm$ 5.787
UKF	<b>180.981<math>\pm</math>1.252</b>	<b>73.284<math>\pm</math>0.483</b>	<b>2.730<math>\pm</math>0.013</b>	<b>0.648<math>\pm</math>0.003</b>	<b>76311.0<math>\pm</math>511.5</b>	<b>181.575<math>\pm</math>3.362</b>
EnKF	$\infty$	$\infty$	$\infty$	$\infty$	$\infty$	$\infty$
PF	363.150 $\pm$ 6.356	108.129 $\pm$ 1.820	4.146 $\pm$ 0.032	1.418 $\pm$ 0.020	138321.6 $\pm$ 2288.0	363.212 $\pm$ 15.790
<i>Neural Models</i>						
GRU	160.496 $\pm$ 4.956	70.828 $\pm$ 3.233	2.675 $\pm$ 0.057	0.549 $\pm$ 0.013	70850.0 $\pm$ 2243.2	159.868 $\pm$ 2.518
LSTM	157.315 $\pm$ 3.946	70.299 $\pm$ 2.629	2.632 $\pm$ 0.063	0.537 $\pm$ 0.013	69968.6 $\pm$ 1599.0	<b>157.712<math>\pm</math>2.009</b>
GPT-2	163.471 $\pm$ 7.896	74.504 $\pm$ 4.286	2.755 $\pm$ 0.123	0.563 $\pm$ 0.018	73587.8 $\pm$ 3813.3	164.351 $\pm$ 3.245
Filterformer	188.368 $\pm$ 4.846	84.899 $\pm$ 3.811	3.152 $\pm$ 0.110	0.648 $\pm$ 0.013	81846.1 $\pm$ 2777.7	189.295 $\pm$ 2.033
Mamba	156.477 $\pm$ 5.064	<b>69.142<math>\pm</math>3.820</b>	<b>2.631<math>\pm</math>0.137</b>	0.540 $\pm$ 0.022	<b>69624.0<math>\pm</math>2822.4</b>	158.369 $\pm$ 3.294
Mamba-2	<b>155.987<math>\pm</math>7.942</b>	70.550 $\pm$ 5.676	2.649 $\pm$ 0.136	<b>0.536<math>\pm</math>0.020</b>	70442.7 $\pm$ 4305.1	158.674 $\pm$ 3.957

Table 12 reports the NRMSE of each method averaged across all scenarios, providing a concise summary of overall performance across different dynamical systems.

**Model-Free Neural State Estimation in Nonlinear Dynamical Systems**

*Table 9.* Extended metrics for L96. Values: median $\pm$ IQR, last column: mean $\pm$ 95%CI.

Method	RMSE	MAE	MedAE	NRMSE	AUC	RMSE (mean $\pm$ 95%CI)
<i>Classical Filters</i>						
EKF	0.049 $\pm$ 0.000	0.027 $\pm$ 0.000	0.013 $\pm$ 0.000	0.014 $\pm$ 0.000	23.7 $\pm$ 0.0	0.049 $\pm$ 0.000
UKF	<b>0.048<math>\pm</math>0.000</b>	<b>0.026<math>\pm</math>0.000</b>	<b>0.013<math>\pm</math>0.000</b>	<b>0.013<math>\pm</math>0.000</b>	<b>23.2<math>\pm</math>0.0</b>	<b>0.048<math>\pm</math>0.000</b>
EnKF	0.054 $\pm$ 0.000	0.029 $\pm$ 0.000	0.013 $\pm$ 0.000	0.015 $\pm$ 0.000	26.1 $\pm$ 0.0	0.054 $\pm$ 0.000
PF	0.065 $\pm$ 0.000	0.037 $\pm$ 0.000	0.018 $\pm$ 0.000	0.018 $\pm$ 0.000	31.6 $\pm$ 0.0	0.065 $\pm$ 0.000
<i>Neural Models</i>						
GRU	0.142 $\pm$ 0.010	0.110 $\pm$ 0.008	0.090 $\pm$ 0.004	0.040 $\pm$ 0.003	69.3 $\pm$ 5.0	0.142 $\pm$ 0.003
LSTM	0.127 $\pm$ 0.005	0.099 $\pm$ 0.005	0.082 $\pm$ 0.004	0.036 $\pm$ 0.002	62.2 $\pm$ 2.7	0.129 $\pm$ 0.003
GPT-2	0.090 $\pm$ 0.030	0.069 $\pm$ 0.029	0.057 $\pm$ 0.032	0.026 $\pm$ 0.009	44.1 $\pm$ 14.7	0.103 $\pm$ 0.011
Filterformer	0.356 $\pm$ 0.013	0.252 $\pm$ 0.006	0.177 $\pm$ 0.004	0.101 $\pm$ 0.003	173.2 $\pm$ 6.3	0.358 $\pm$ 0.005
Mamba	<b>0.052<math>\pm</math>0.001</b>	<b>0.031<math>\pm</math>0.001</b>	<b>0.017<math>\pm</math>0.001</b>	<b>0.015<math>\pm</math>0.000</b>	<b>25.3<math>\pm</math>0.5</b>	<b>0.052<math>\pm</math>0.001</b>
Mamba-2	0.053 $\pm$ 0.002	0.032 $\pm$ 0.002	0.018 $\pm$ 0.001	0.015 $\pm$ 0.001	25.9 $\pm$ 0.9	0.054 $\pm$ 0.001

*Table 10.* Extended metrics for Nlink Pendulum. Values: median $\pm$ IQR, last column: mean $\pm$ 95%CI.

Method	RMSE	MAE	MedAE	NRMSE	AUC	RMSE (mean $\pm$ 95%CI)
<i>Classical Filters</i>						
EKF	<b>0.090<math>\pm</math>0.000</b>	<b>0.069<math>\pm</math>0.000</b>	<b>0.057<math>\pm</math>0.000</b>	<b>0.030<math>\pm</math>0.000</b>	<b>44.1<math>\pm</math>0.1</b>	<b>0.090<math>\pm</math>0.001</b>
UKF	0.097 $\pm$ 0.001	0.070 $\pm$ 0.000	0.058 $\pm$ 0.000	0.031 $\pm$ 0.000	46.7 $\pm$ 0.5	0.097 $\pm$ 0.003
EnKF	0.125 $\pm$ 0.001	0.092 $\pm$ 0.000	0.073 $\pm$ 0.000	0.041 $\pm$ 0.000	60.7 $\pm$ 0.3	0.126 $\pm$ 0.002
PF	1.008 $\pm$ 0.022	0.188 $\pm$ 0.003	0.066 $\pm$ 0.000	0.311 $\pm$ 0.006	378.2 $\pm$ 10.2	1.016 $\pm$ 0.056
<i>Neural Models</i>						
GRU	0.270 $\pm$ 0.038	0.154 $\pm$ 0.007	0.110 $\pm$ 0.005	0.084 $\pm$ 0.010	115.9 $\pm$ 11.7	0.281 $\pm$ 0.020
LSTM	0.214 $\pm$ 0.042	0.126 $\pm$ 0.006	0.097 $\pm$ 0.004	0.066 $\pm$ 0.012	93.3 $\pm$ 13.2	0.220 $\pm$ 0.019
GPT-2	0.247 $\pm$ 0.056	0.128 $\pm$ 0.011	0.094 $\pm$ 0.008	0.075 $\pm$ 0.016	101.0 $\pm$ 16.6	0.248 $\pm$ 0.022
Filterformer	0.294 $\pm$ 0.040	0.156 $\pm$ 0.009	0.111 $\pm$ 0.007	0.093 $\pm$ 0.012	132.4 $\pm$ 15.7	0.297 $\pm$ 0.017
Mamba	0.172 $\pm$ 0.032	<b>0.070<math>\pm</math>0.004</b>	<b>0.058<math>\pm</math>0.003</b>	<b>0.051<math>\pm</math>0.009</b>	66.7 $\pm$ 11.1	<b>0.168<math>\pm</math>0.017</b>
Mamba-2	<b>0.171<math>\pm</math>0.041</b>	0.071 $\pm$ 0.005	0.058 $\pm$ 0.003	0.052 $\pm$ 0.013	<b>65.3<math>\pm</math>10.2</b>	0.168 $\pm$ 0.026

*Table 11.* Extended metrics for Planar Quadrotor. Values: median $\pm$ IQR, last column: mean $\pm$ 95%CI.

Method	RMSE	MAE	MedAE	NRMSE	AUC	RMSE (mean $\pm$ 95%CI)
<i>Classical Filters</i>						
EKF	<b>0.273<math>\pm</math>0.001</b>	<b>0.125<math>\pm</math>0.000</b>	<b>0.041<math>\pm</math>0.000</b>	<b>0.007<math>\pm</math>0.000</b>	<b>51.2<math>\pm</math>0.2</b>	<b>0.272<math>\pm</math>0.003</b>
UKF	8.112 $\pm$ 0.324	0.988 $\pm$ 0.029	0.054 $\pm$ 0.000	0.068 $\pm$ 0.004	1223.4 $\pm$ 45.0	8.256 $\pm$ 0.862
EnKF	9.726 $\pm$ 0.198	1.738 $\pm$ 0.018	0.092 $\pm$ 0.001	0.083 $\pm$ 0.004	1501.8 $\pm$ 27.0	9.828 $\pm$ 0.537
PF	113.424 $\pm$ 3.570	38.262 $\pm$ 0.084	1.302 $\pm$ 0.009	0.898 $\pm$ 0.009	16098.9 $\pm$ 371.5	113.770 $\pm$ 8.900
<i>Neural Models</i>						
GRU	36.423 $\pm$ 12.976	6.305 $\pm$ 0.812	1.562 $\pm$ 0.270	0.201 $\pm$ 0.059	4330.8 $\pm$ 1122.7	34.192 $\pm$ 5.323
LSTM	35.205 $\pm$ 12.625	6.275 $\pm$ 0.598	1.381 $\pm$ 0.221	0.198 $\pm$ 0.053	4223.1 $\pm$ 1074.9	32.062 $\pm$ 3.943
GPT-2	64.994 $\pm$ 9.601	8.082 $\pm$ 1.197	1.864 $\pm$ 0.570	0.239 $\pm$ 0.037	6873.7 $\pm$ 1288.1	65.907 $\pm$ 4.509
Filterformer	41.504 $\pm$ 12.962	7.308 $\pm$ 0.639	1.562 $\pm$ 0.199	0.225 $\pm$ 0.051	4672.7 $\pm$ 1077.2	38.256 $\pm$ 3.798
Mamba	<b>31.768<math>\pm</math>18.593</b>	2.995 $\pm$ 0.580	0.635 $\pm$ 0.078	0.164 $\pm$ 0.083	<b>3327.6<math>\pm</math>1658.1</b>	<b>27.011<math>\pm</math>5.323</b>
Mamba-2	33.925 $\pm$ 14.224	<b>2.614<math>\pm</math>0.902</b>	<b>0.573<math>\pm</math>0.139</b>	<b>0.159<math>\pm</math>0.066</b>	3334.1 $\pm$ 1284.7	30.422 $\pm$ 6.723

*Table 12.* NRMSE averaged over all scenarios. Lower is better.

Metric	Classical Filters				Neural Models					
	EKF	UKF	EnKF	PF	GRU	LSTM	GPT-2	Filterformer	Mamba	Mamba-2
Avg. NRMSE (IQR)	<b>0.030</b> (0.995)	0.068 (0.574)	0.083 (0.855)	0.643 (0.587)	0.201 (0.465)	0.198 (0.472)	0.239 (0.489)	0.225 (0.547)	0.164 (0.489)	<b>0.159</b> (0.485)